

Supporting Information

Small molecular donor materials based on β - β -bridged BODIPY dimers with triphenylamine or carbazole unit for efficient organic solar cells

Minhao Zhu,^a Tingting Gu,^a Xu Liang^b, Sarvesh Kumar Pandey^c, Claude P. Gros^d,
Hai-Jun Xu,^{a,e*} and Ganesh D. Sharma^{f*}

Table of contents

Experimental Procedures. Synthesis		p. 3
X-ray diffraction patterns		p. 5
Device fabrication and characterization		p. 6
Figure S1.	¹ H-NMR spectrum (400 MHz, 298 K) of compound a in CDCl ₃	p. 8
Figure S2.	¹³ C-NMR spectrum (151 MHz, 298 K) of compound a in CDCl ₃	p. 8
Figure S3.	High resolution ESI-Mass Spectrum of compound a	p. 9
Figure S4.	¹ H-NMR spectrum (400 MHz, 298 K) of compound b in CDCl ₃	p. 9
Figure S5.	¹³ C-NMR spectrum (151 MHz, 298 K) of compound b in CDCl ₃	p. 10
Figure S6.	High resolution ESI-Mass Spectrum of compound b	p. 10
Figure S7.	¹ H-NMR spectrum (600 MHz, 298 K) of compound ZMH-1 in CDCl ₃	p. 11
Figure S8.	¹³ C-NMR spectrum (151 MHz, 298 K) of compound ZMH-1 in CDCl ₃	p. 11
Figure S9.	¹ H-NMR spectrum (600 MHz, 298 K) of compound ZMH-2 in CDCl ₃	p. 12
Figure S10.	¹³ C-NMR spectrum (151 MHz, 298 K) of compound ZMH-2 in CDCl ₃	p. 12
Figure S11.	MALDI-TOF-MS spectrum of compound ZMH-1	p. 13
Figure S12.	MALDI-TOF-MS spectrum of compound ZMH-2	p. 13
Figure S13.	High resolution ESI-Mass Spectrum of compound ZMH-1	p. 14
Figure S14.	High resolution ESI-Mass Spectrum of compound ZMH-2	p. 15
Figure S15.	TG diagram thermogravimetric analysis of compound (a) ZMH-1 and (b) ZMH-2	p. 16

Figure S16.	DSC diagram analysis of compound (a) ZMH-1 and (b) ZMH-2	p. 16
Figure S17.	(a) UV-visible absorption spectrum and (b) PL spectra of compounds ZMH-1 and ZMH-2 in CH ₂ Cl ₂	p. 17
Figure S18.	Cyclic voltammograms of compound (a) ZMH-1 and (b) ZMH-2 in <i>o</i> -DCB containing 0.1 M TBAP at scan speed of 0.1 V/s	p. 17
Figure S19.	Optimized structures of ZMH-1 and ZMH-2	p. 18
Figure S20.	X-ray diffraction patterns of compound ZMH-1 and ZMH-2	p. 18
Figure S21.	(a) J-V characteristics under illumination and (b) EQE spectra (ZMH-1 and ZMH-2 as donor and PC ₇₁ BM as acceptor)	p. 19
Figure S22.	Dark J-V characteristics for the electron (left) and hole (right) only devices and their SCLC fitting	p. 19
Figure S23.	TRPL decay spectra for (a) pristine ZMH-1 and its binary and ternary blends, and (b) ZMH-2 and its binary and ternary blends	p. 20
Table S1a.	Photovoltaic parameters of the OSCs using ZMH-1 : IDT-TC BHJ active layer with different weight ratios of ZMH-1 donor	p. 20
Table S1b.	Photovoltaic parameters of the OSCs using ZMH-2 : IDT-TC BHJ active layer with different weight ratios of ZMH-2 donor	p. 20
Table S2a.	Photovoltaic parameters of OSCs based on ternary ZMH-1 :PC ₇₁ BM:IDT-TC with different weight ratios between PC ₇₁ BM and IDT-TC	p. 20
Table S2b.	Photovoltaic parameters of OSCs based on ternary ZMH-2 :PC ₇₁ BM:IDT-TC with different weight ratios between PC ₇₁ BM and IDT-TC	p. 21

Synthesis (Experimental Procedures)

1.1. Synthesis of **a**

2,4,6-Trimethylbenzaldehyde (5 mmol, 0.73 mL) and 2-methylpyrrole (11 mmol, 810 mg) were dissolved in CH₂Cl₂ (250 mL) under argon. Trifluoroacetic acid (50 μ L) was added to the mixture after stirring for 10 min at room temperature shielded from light. The reaction solution was left stirred at room temperature overnight. After addition of 2,3-dichloro-5,6-dicyano-4-benzoquinone (5 mmol, 1.135 g), the argon gas was removed and the reaction mixture was stirred at room temperature for another 3 h. Triethylamine (10 mL) and boron trifluoride ether (10 mL) were then slowly added to the reaction solution under an ice bath, and the reaction mixture was then warmed up slowly to room temperature for 3 h. The solvent was removed under reduced pressure, and the residue was purified by silica gel column chromatography with CH₂Cl₂/petroleum ether (v/v = 1:3) as eluent to afford compound **a** (1.21 g, 66% yield) as an orange solid. ¹H NMR (CDCl₃, 400 MHz): δ (ppm) 6.92 (s, 2H), 6.46 (d, J = 3.2 Hz, 2H), 6.19-6.18 (m, 2H), 2.64 (s, 6H), 2.34 (s, 3H), 2.10 (s, 6H). ¹³C NMR (CDCl₃, 151 MHz): δ (ppm) 157.5, 142.3, 138.3, 136.6, 134.7, 130.0, 129.6, 129.0, 128.0, 119.3, 21.1, 19.9, 14.9. ESI-HRMS: calculated for C₂₀H₂₁BF₂N₂: 361.1664; found: 361.1672 [M+Na]⁺.

1.2. Synthesis of **b**

Under nitrogen, compound **a** (134 mg, 0.4 mmol) was dissolved in dry CH₂Cl₂ (100 mL), and then a CH₃NO₂ (3.6 mL) solution of FeCl₃ (194 mg, 1.2 mmol) was added dropwise at -78°C. After half an hour, the mixture was quenched by addition of MeOH (50 mL) and then stirred for an additional 30 min. The organic phase was washed with H₂O (2 \times 50 mL), dried over Na₂SO₄. The solvent was then concentrated under reduced pressure, and the crude product was purified by silica gel column chromatography using CH₂Cl₂/petroleum ether (v/v = 1:1) as eluent to afford compound **b** (191 mg, 57% yield) as a dark green solid. ¹H NMR (CDCl₃, 400 MHz): δ (ppm) 6.92 (s, 4H), 6.48-6.20 (m, 6H), 2.64 (s, 6H), 2.52 (s, 6H), 2.34 (s, 6H), 2.11 (s, 12H). ¹³C NMR (CDCl₃, 151 MHz): δ (ppm) 158.3, 155.6, 142.0, 138.4, 136.6, 135.1, 133.7, 130.6, 129.9, 129.3, 128.1, 126.6, 119.7, 21.0, 20.0, 15.0, 13.4. ESI-HRMS: calculated for C₄₀H₄₀B₂F₄N₄: 697.3273;

found: 697.3265 [M+Na]⁺.

1.3. Synthesis of **ZMH-1**

Compound **b** (33.7 mg, 0.05 mmol), 4-(*N,N*-diphenylamino)benzaldehyde (68 mg, 0.25mmol), *p*-toluenesulfonic acid (PTSA, 10 mg, 0.05 mmol) was dissolved in dry toluene (10 mL), and piperidine (0.2 mL) was added. A Dean-Stark device was used and the reaction mixture was heated to 140 °C under stirring. After the reaction of the raw material was complete, the residual toluene was evaporated through the Dean-Stark device. The mixture was extracted with CH₂Cl₂, and the combined organic phases were washed with water. The solvent was then concentrated under reduced pressure, and the crude product was purified by silica gel column chromatography using CH₂Cl₂/petroleum ether (v/v = 1:1) as eluent to afford compound **ZMH-1** (58 mg, 69% yield) as a black solid. ¹H NMR (CDCl₃, 600 MHz): δ (ppm) 7.64-7.57 (m, 4H), 7.47 (d, *J* = 9 Hz, 4H), 7.30-7.27 (m, 10H), 7.24-7.23 (m, 10H), 7.14 (d, *J* = 7.8 Hz, 8H), 7.10-7.06 (m, 14H), 7.04-7.02 (m, 10H), 6.93 (d, *J* = 8.4 Hz, 4H), 6.88 (s, 4H), 6.85 (d, *J* = 4.2 Hz, 2H), 6.52 (d, *J* = 4.2 Hz, 2H), 6.42 (s, 2H), 2.31 (s, 6H), 2.10 (s, 12H). ¹³C NMR (CDCl₃, 151 MHz): δ (ppm) 155.6, 150.9, 149.4, 148.9, 148.5, 147.2, 147.1, 138.2, 137.3, 136.8, 136.7, 130.8, 130.3, 130.0, 129.4, 129.3, 128.7, 128.5, 128.2, 128.1, 125.2, 124.9, 123.7, 123.4, 122.4, 122.2, 117.3, 117.1, 117.1, 116.7, 116.7, 116.7, 116.0, 21.1, 20.1. MALDI-TOF MS [M-F]⁻ calculated for C₁₁₆H₉₂B₂F₃N₈: 1675.758; found: 1675.634. ESI-HRMS: calculated for C₁₁₆H₉₂B₂F₄N₈: 1694.7567; found: 1695.7618 [M]⁺.

1.4. Synthesis of **ZMH-2**

Compound **b** (50 mg, 0.074 mmol), 9-butyl-9H-carbazole-3-carbaldehyde (93 mg, 0.37mmol), *p*-toluenesulfonic acid (PTSA, 13 mg, 0.074 mmol) was dissolved in dry toluene (10 mL), and piperidine (0.2 mL) was added. A Dean-Stark device was used and the reaction mixture was heated to 140 °C under stirring.. After the reaction of the raw material was complete, the residual toluene was evaporated using the Dean-Stark device. The mixture was extracted with CH₂Cl₂, and the combined organic phase was washed with water. The solvent was then concentrated under reduced pressure, and the crude product was purified by silica gel column chromatography using

CH₂Cl₂/petroleum ether (v/v = 1:1) as eluent to afford compound **ZMH-2** (80 mg, 67% yield) as a black solid. ¹H NMR (CDCl₃, 600 MHz): δ (ppm) 8.38 (s, 2H), 8.22-8.20 (m, 4H), 8.15 (d, *J* = 7.8 Hz, 2H), 7.95-7.85 (m, 6H), 7.64-7.62 (m, 4H), 7.53-7.50 (m, 4H), 7.47-7.43 (m, 6H), 7.38-7.33 (m, 4H), 7.30-7.28 (m, 2H), 7.23-7.20 (m, 2H), 6.99-6.98 (m, 2H), 6.86 (s, 4H), 6.60 (d, *J* = 4.8 Hz, 2H), 6.56 (s, 2H), 4.34 (t, *J* = 7.2 Hz, 4H), 4.26 (t, *J* = 7.2 Hz, 4H), 2.28 (s, 6H), 2.16(s, 12H), 1.91-1.83 (m, 8H), 1.46-1.42 (m, 4H), 1.40-1.36 (m, 4H). ¹³C NMR (CDCl₃, 151 MHz): δ (ppm) 155.9, 154.9, 153.1, 151.7, 151.5, 150.7, 150.6, 148.9, 141.3, 141.1, 140.9, 140.8, 139.5, 139.1, 138.6, 138.2, 137.9, 136.9, 130.4, 128.3, 128.1, 128.1, 127.9, 126.0, 126.0, 125.7, 123.4, 123.2, 123.0, 122.9, 120.9, 120.6, 120.1, 119.5, 119.2, 116.7, 116.3, 109.2, 109.0, 108.9, 108.8, 43.0, 42.9, 31.1, 31.1, 21.0, 20.6, 20.5, 20.1, 13.9, 13.8. MALDI-TOF MS [M-F]⁻ calculated for C₁₀₈H₁₀₀B₂F₃N₈: 1587.821; found: 1587.674. ESI-HRMS: calculated for C₁₀₈H₁₀₀B₂F₄N₈: 1606.8193; found: 1606.8218 [M]⁺.

2.1. X-ray diffraction patterns

To obtain information about the molecular packing of the crystallinity, we have recorded the X-ray diffraction patterns of compounds **ZMH-1** and **ZMH-2** as shown in Fig. S14-15. Both **ZMH-1** and **ZMH-2** show two diffraction peaks with different values of 2θ . One of the two diffraction peaks appears at $2\theta = 13.38^\circ$ and 13.18° for **ZMH-1** and **ZMH-2** with lamellar distances of 0.661 and 0.671 nm, respectively, and the other at $2\theta = 20.72^\circ$ and 19.32° for **ZMH-1** and **ZMH-2** with the π - π stacking distances of 0.428 and 0.459, respectively. As can be seen, the intensity of the diffraction peak is stronger than that for **ZMH-2**, which indicates that the crystal coherence length (CCL) for diffraction for **ZMH-1** is higher than that for **ZMH-2**. The higher value of CCLs is beneficial for the charge transport, leading to the suppression of charge recombination, resulting to higher value of FF for **ZMH-1** OSC as compared to **ZMH-2**.

Device fabrication and characterization

The solution processed organic solar cells were fabricated on the ITO coated glass substrate with structure ITO/PESOT:PSS/active layer /PFN/Al. The ITO coated glass substrates were cleaned in detergent, and subsequently ultra-sonicated in deionized water, acetone and isopropyl alcohol and dried *in vacuum* oven to remove all the traces of residues. We have fabricated devices using **ZMH-1** and **ZMH-2** as donor and two acceptors i.e., PC₇₁BM and IDT-TC NFA. The photovoltaic performance optimization process was started with identifying the donor to acceptor ratio and after that solvent vapor annealing was applied to maximize the performance of the OSCs. The total concentration of D:A blend mixture was 16 mg/mL in chloroform. The devices were fabricated by depositing PEDOT:PSS as hole transport layer having thickness of 35-40 nm. The active layer was deposited by spin coating (2500 rpm, 60 s) on the top of PEDOT:PSS layer under ambient conditions. After that we have optimize the device performance via solvent vapor treatment (SVA) method. The active layer with optimized weight ratio was exposed to the THF vapours for 40s. A thin layer of PFN was spin coated on the top of the active layer from the methanol solution. The aluminium (Al) electrode was deposited onto the top of PFN layer *via* thermal evaporation at the pressure less than 10⁻⁵ Torr. All devices were fabricated and tested in an ambient atmosphere without encapsulation. The effective area of the devices is 0.16 cm². The ternary OSCs were fabricated via varying the weight ratio between two acceptors (PC₇₁BM and IDT-TC) and keeping the concentration of **ZMH-1** or **ZMH-2** donor constant. The optimization is done same as for binary counterparts. The current-voltage characteristics of the OSCs were measured under illumination intensity of 100 mW/cm² (AM1.5 G) using a solar simulator and a Keithley 2400 source meter unit. The External quantum efficiency (EQE) measurements were performed using Bentham EQE system. The hole-only and electron-only devices with ITO/PEDOT:PSS/active layer /Au and ITO/Al/ active layer/Al architectures were also fabricated in a similar way, to measure the hole and electron mobility. We have measured the dark J-V characteristics and fitted with the space charge limited current model.

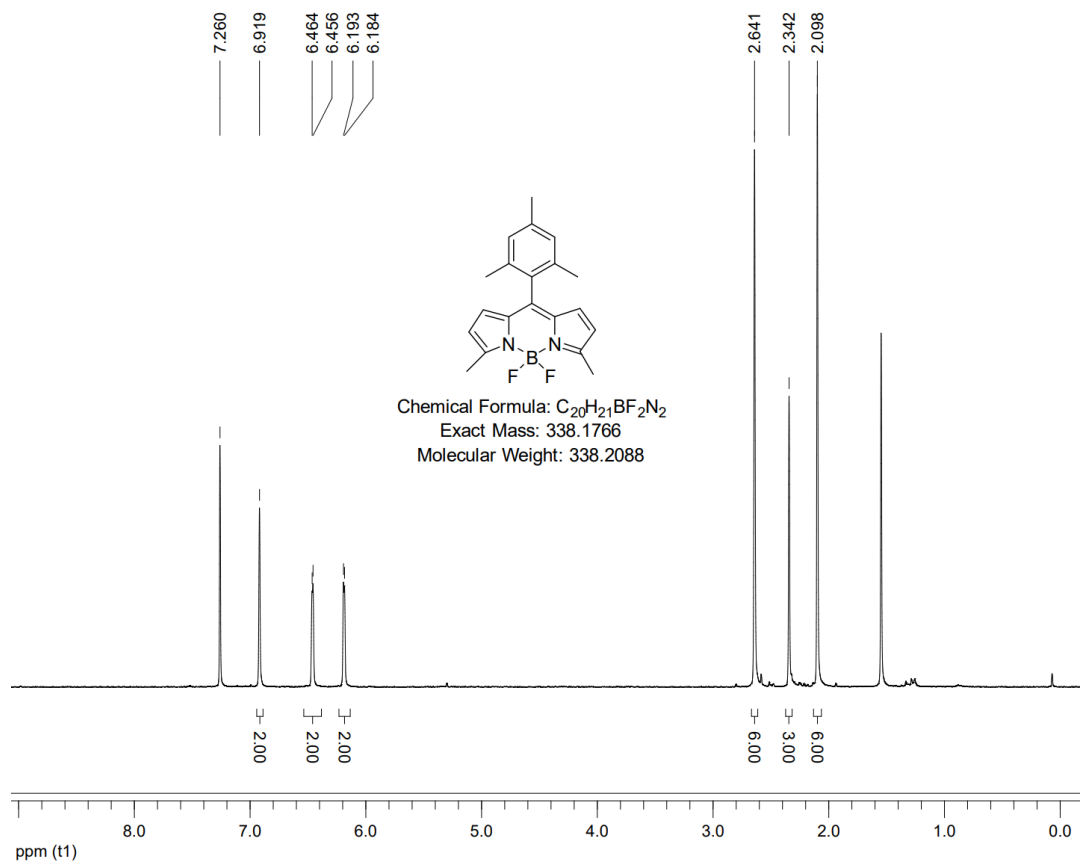


Figure S1. 1H -NMR spectrum (400 MHz, 298 K) of compound **a** in $CDCl_3$

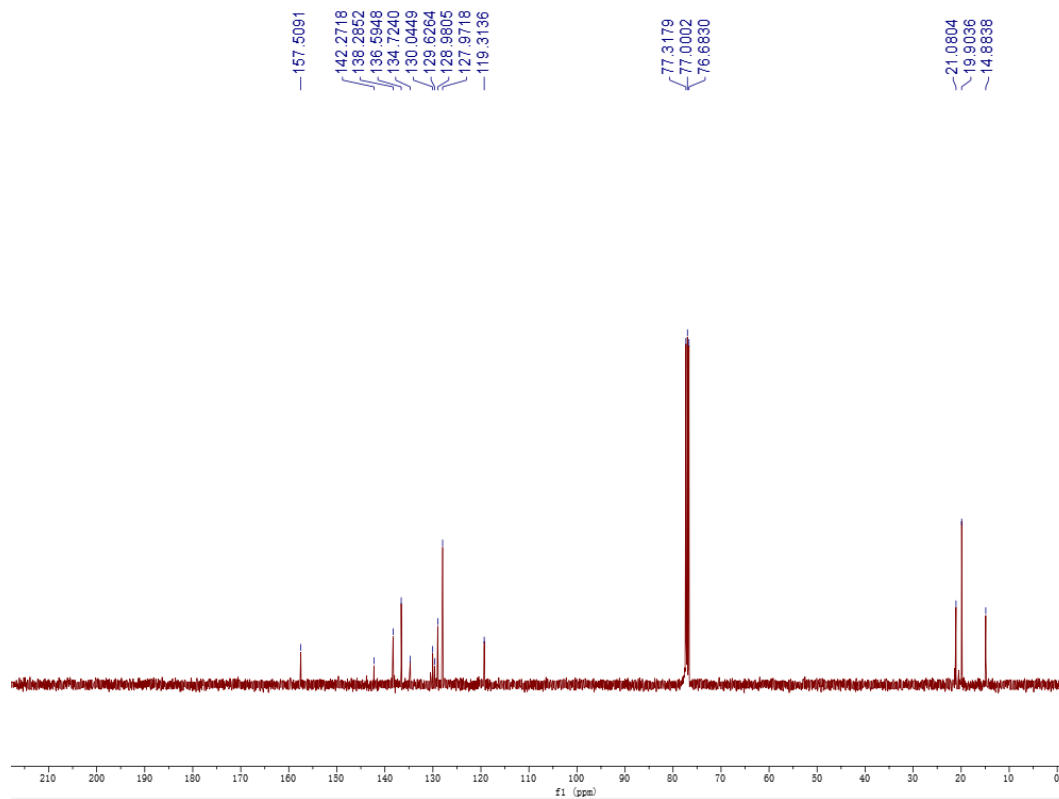
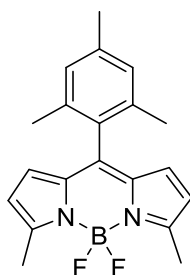
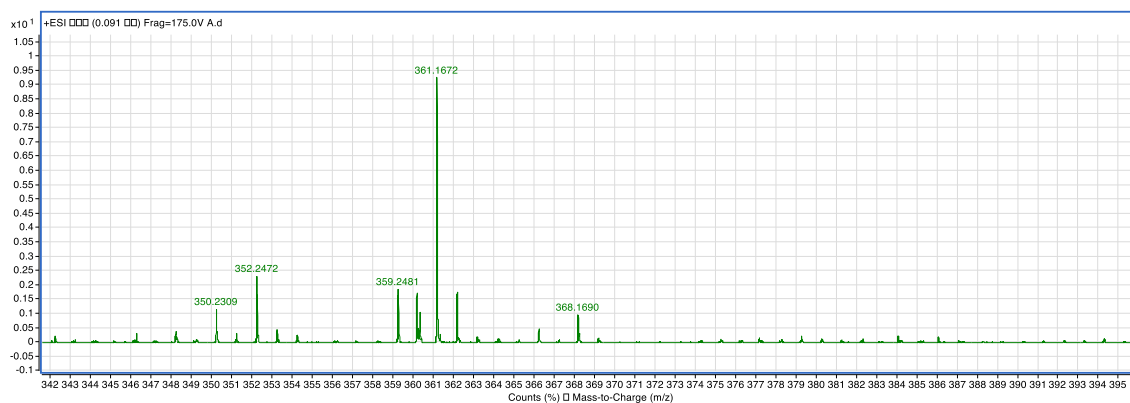


Figure S2. ^{13}C -NMR spectrum (151 MHz, 298 K) of compound **a** in $CDCl_3$



Chemical Formula: $C_{20}H_{21}BF_2N_2$

Exact Mass: 338.1766

Molecular Weight: 338.2088

a

Figure S3. High resolution ESI-Mass Spectrum of compound **a**

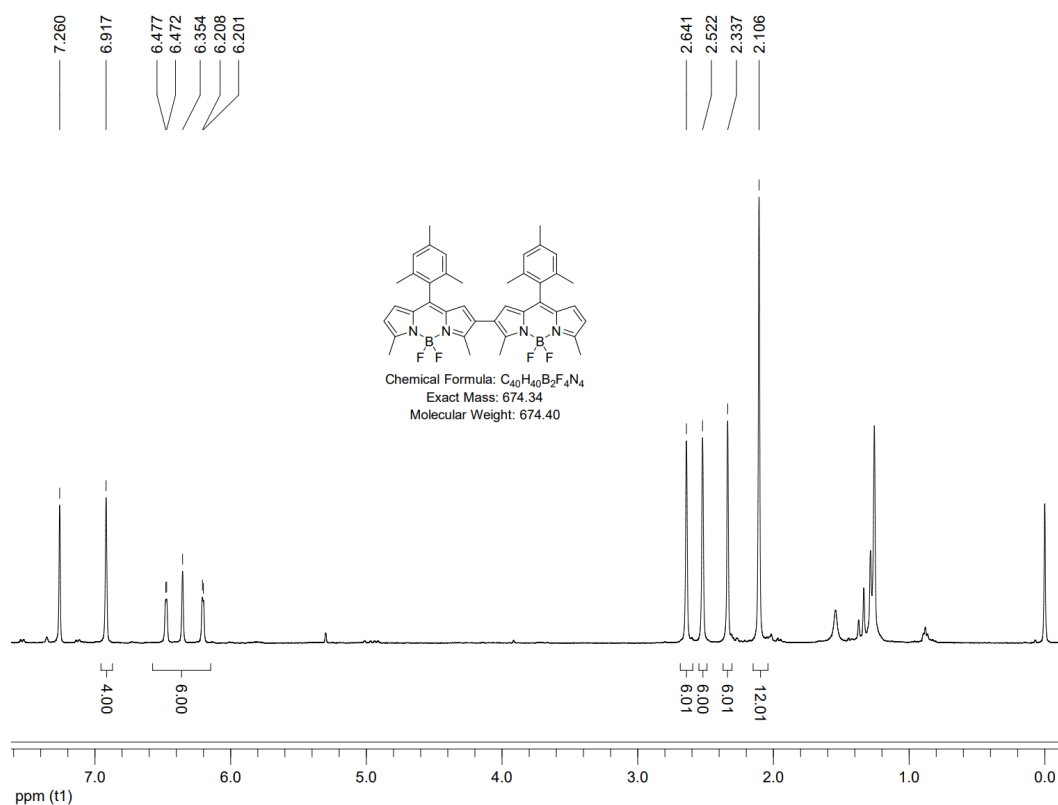


Figure S4. 1H -NMR spectrum (400 MHz, 298 K) of compound **b** in $CDCl_3$

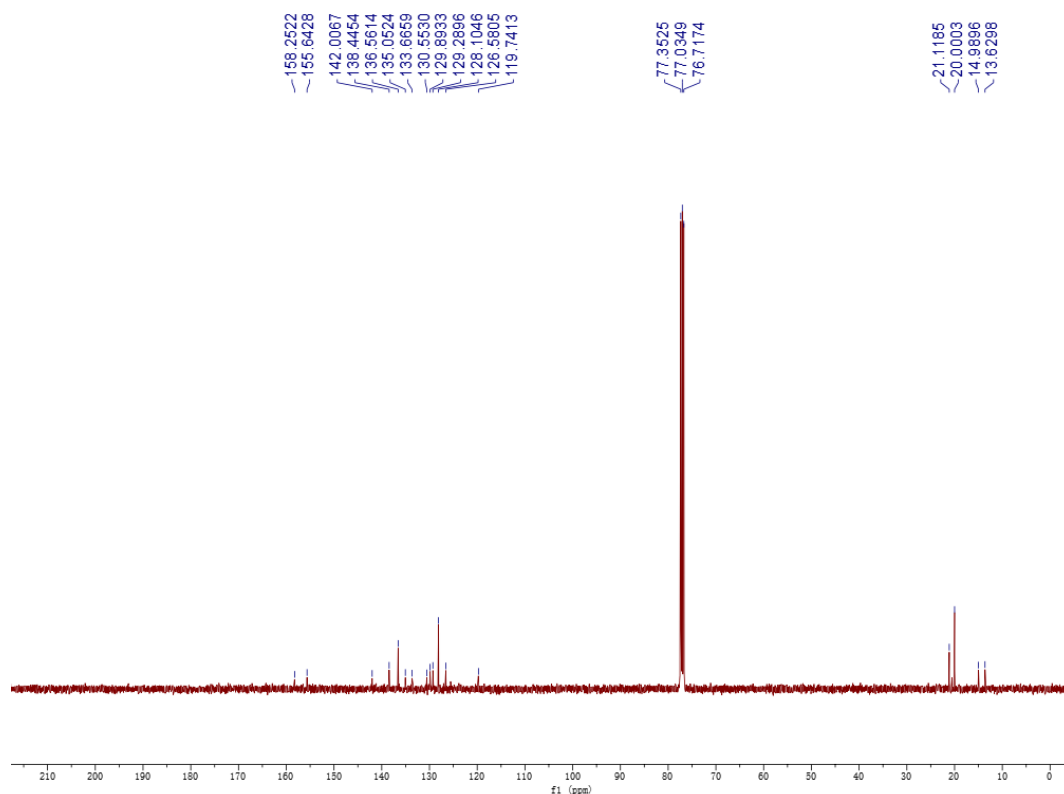
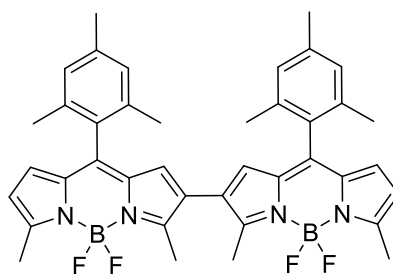
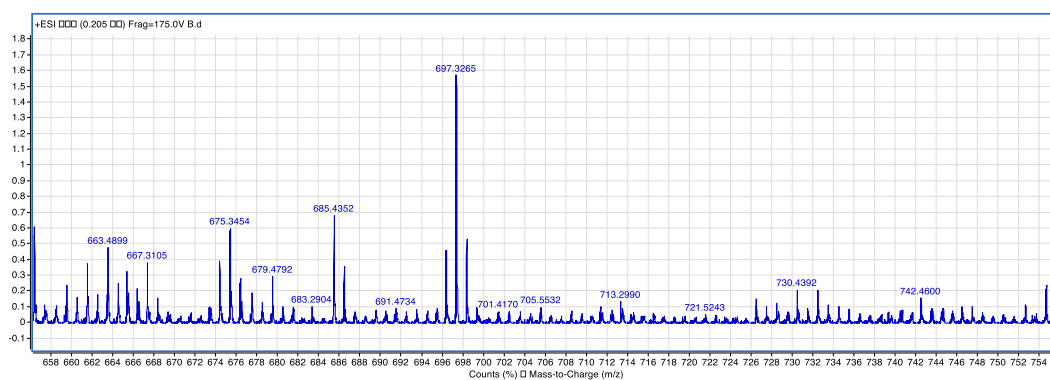


Figure S5. ^{13}C -NMR spectrum (151 MHz, 298 K) of compound **b** in CDCl_3



Chemical Formula: $\text{C}_{40}\text{H}_{40}\text{B}_2\text{F}_4\text{N}_4$

Exact Mass: 674.3375

Molecular Weight: 674.4016

b

Figure S6. High resolution ESI-Mass Spectrum of compound **b**

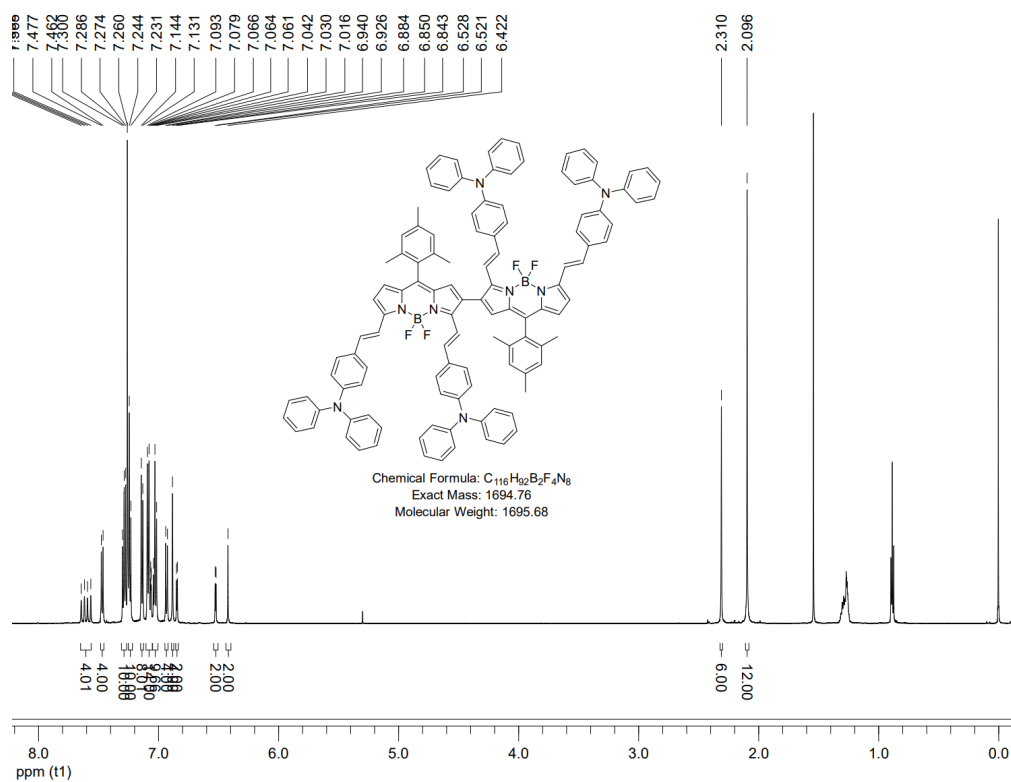


Figure S7. ^1H -NMR spectrum (600 MHz, 298 K) of compound **ZMH-1** in CDCl_3

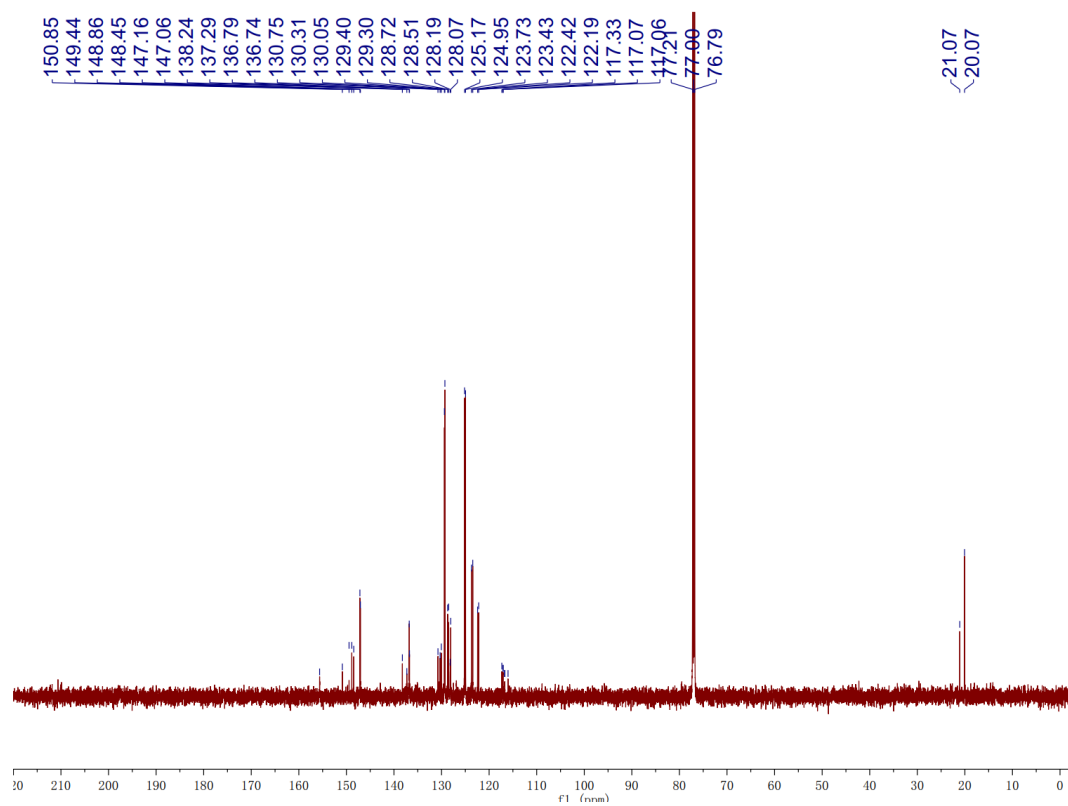


Figure S8. ^{13}C -NMR spectrum (151 MHz, 298 K) of compound **ZMH-1** in CDCl_3

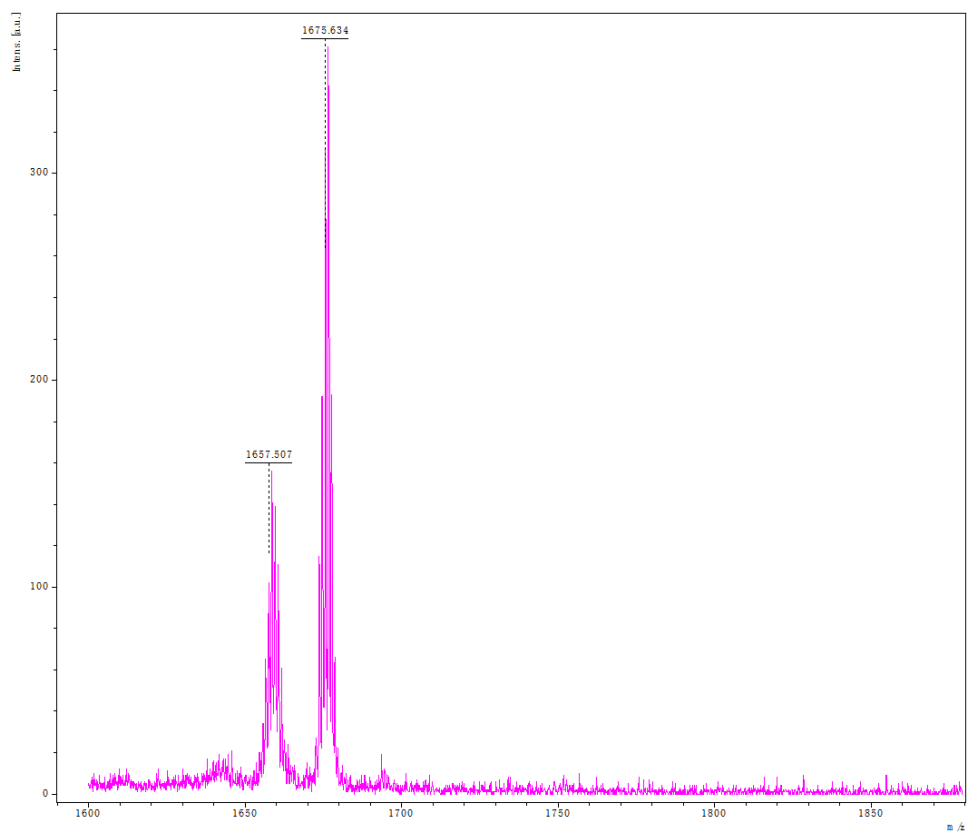


Figure S11. MALDI-TOF-MS spectrum of compound **ZMH-1**

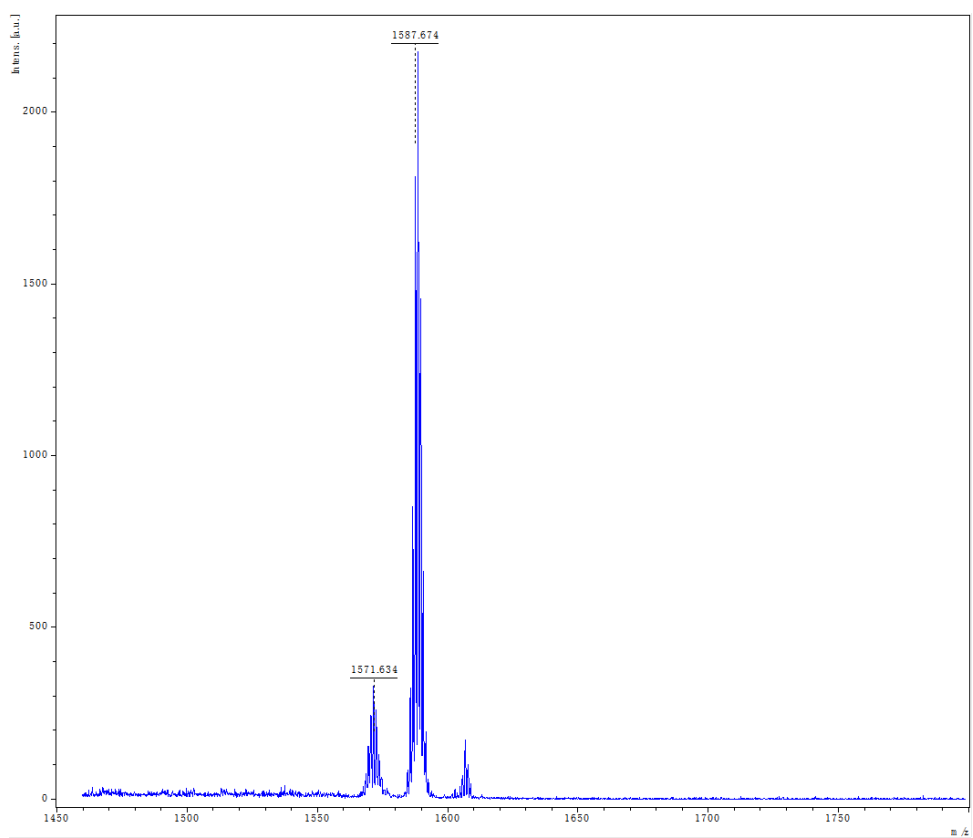


Figure S12. MALDI-TOF-MS spectrum of compound **ZMH-2**

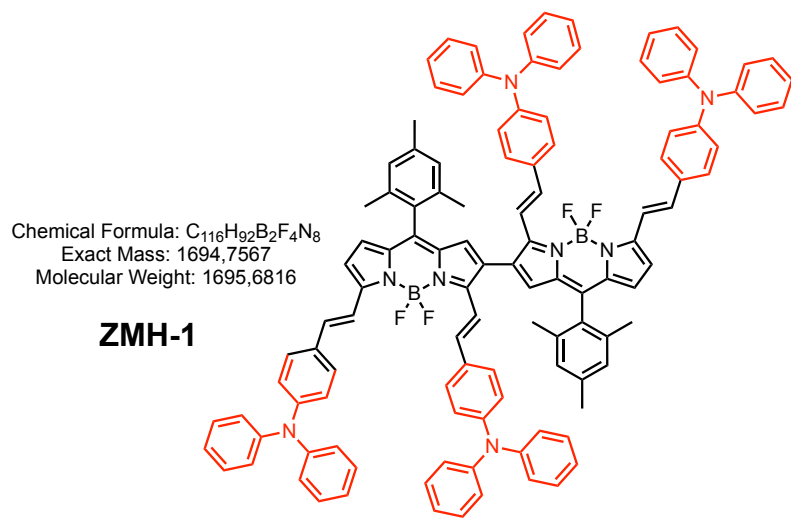
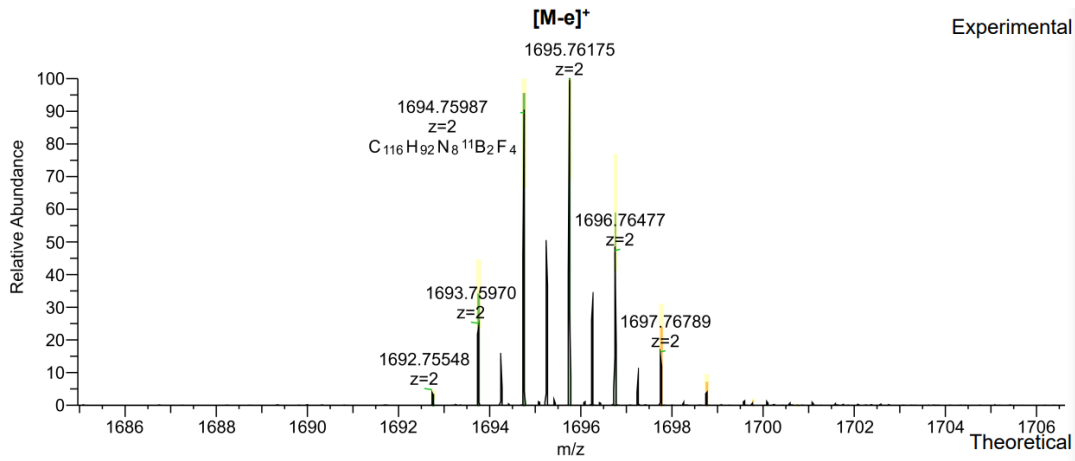
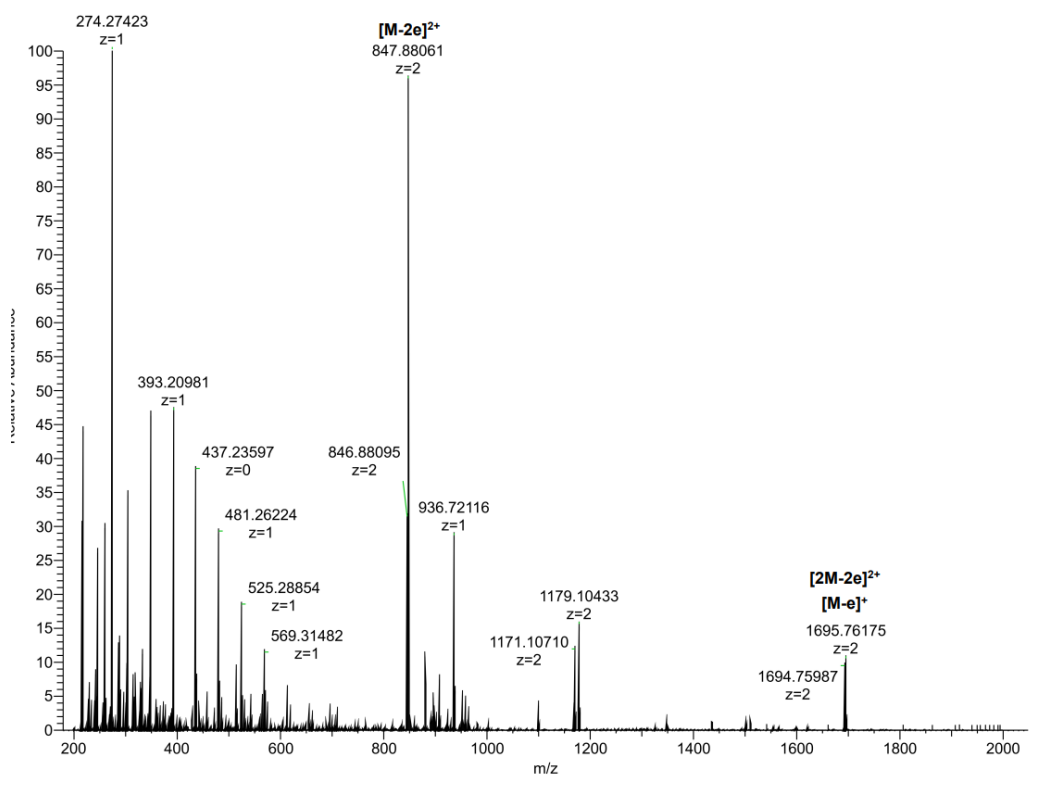


Figure S13. High resolution ESI-Mass Spectrum of compound **ZMH-1**

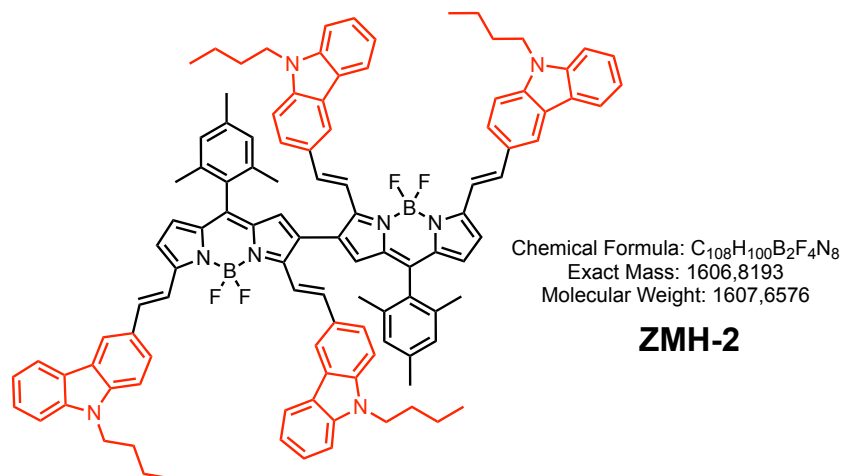
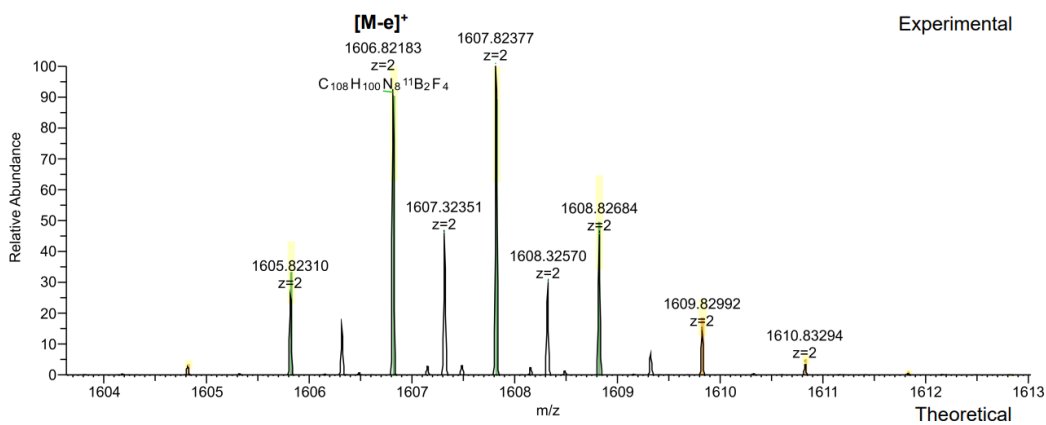
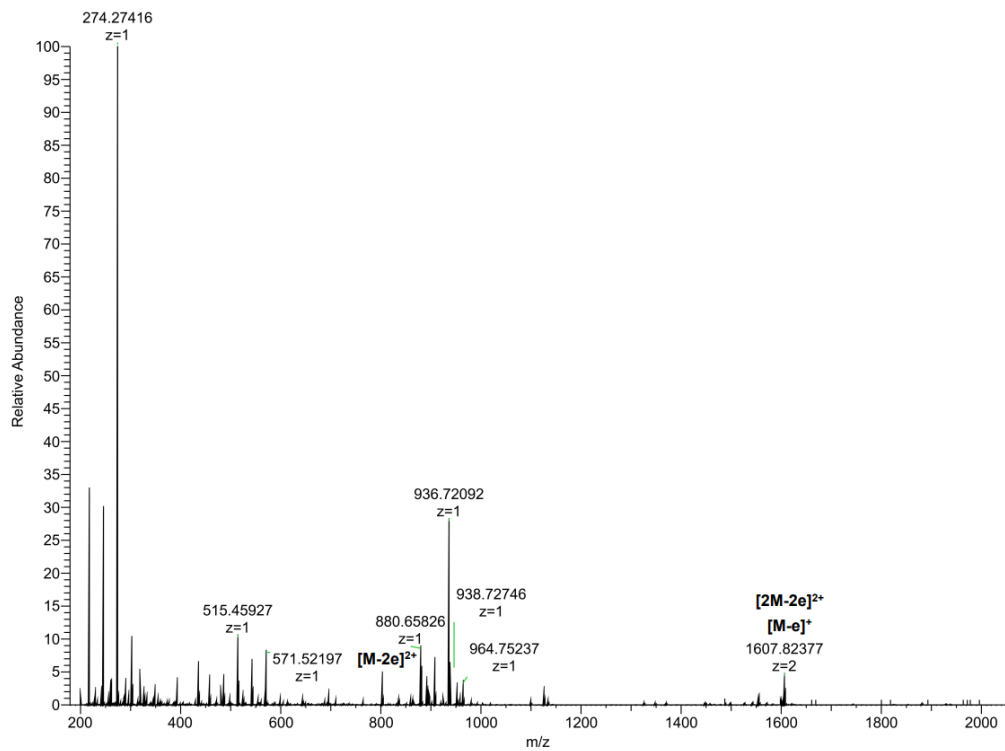
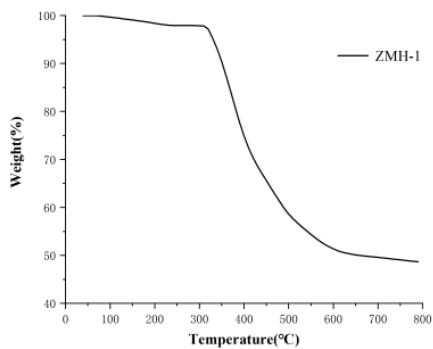
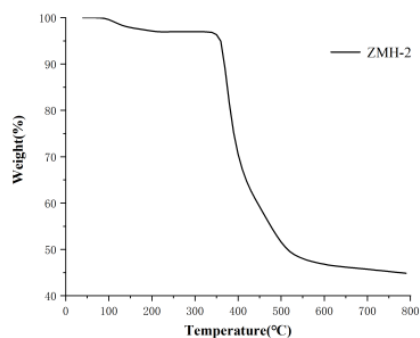


Figure S14. High resolution ESI-Mass Spectrum of compound **ZMH-2**

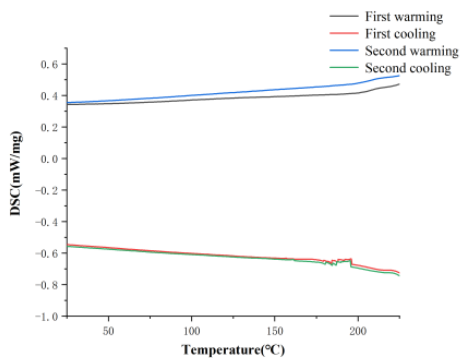


(a)

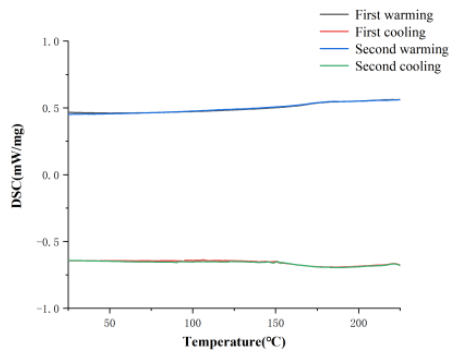


(b)

Figure S15. TGA diagram thermogravimetric analysis of compound (a) **ZMH-1** and (b) **ZMH-2**



(a)



(b)

Figure S16. DSC diagram analysis of compound (a) **ZMH-1** and (b) **ZMH-2**

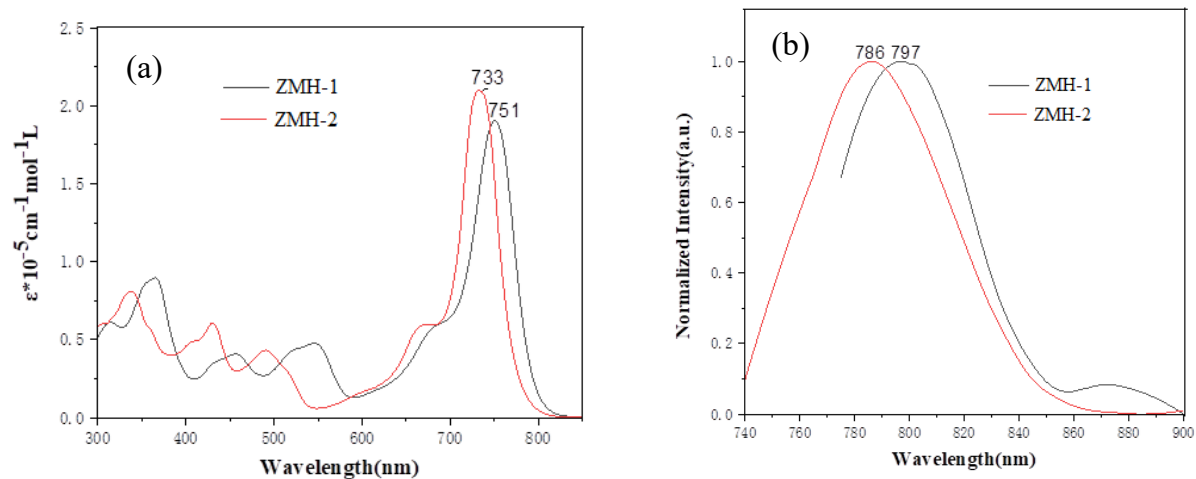


Figure S17. (a) UV-visible absorption spectra and (b) PL spectra of compounds **ZMH-1** and **ZMH-2** in CH_2Cl_2

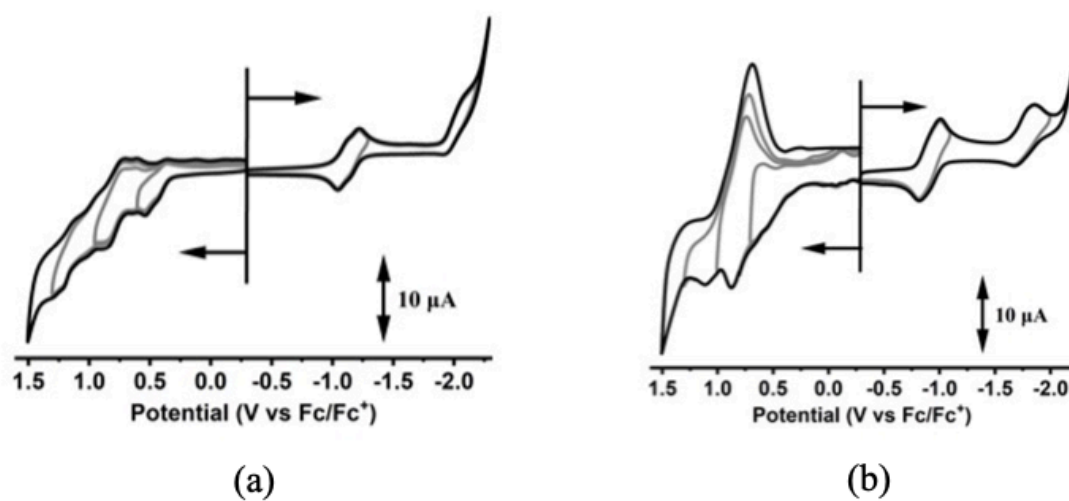


Figure S18. Cyclic voltammograms of compound (a) **ZMH-1** and (b) **ZMH-2** in *o*-DCB containing 0.1 M TBAP at scan speed of 0.1 V/s

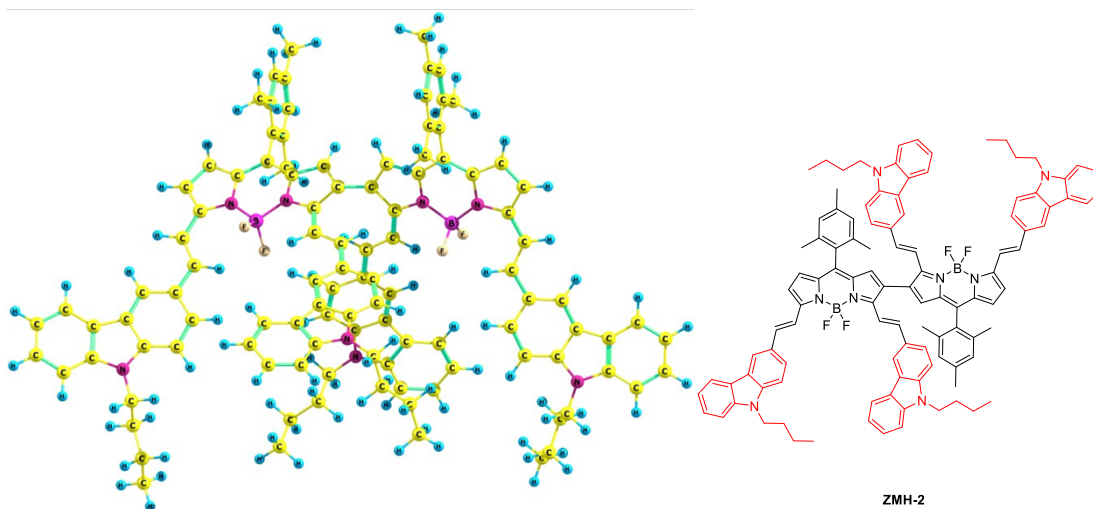
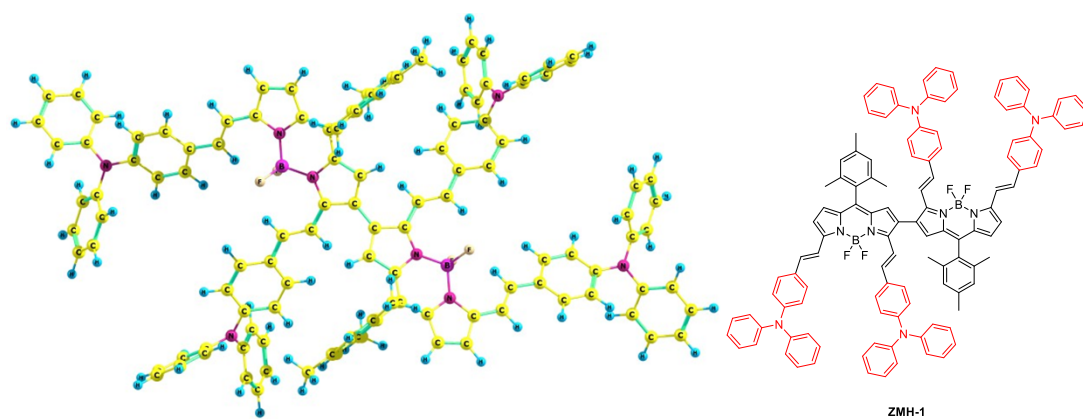


Figure S19. Optimized structures of **ZMH-1** and **ZMH-2**

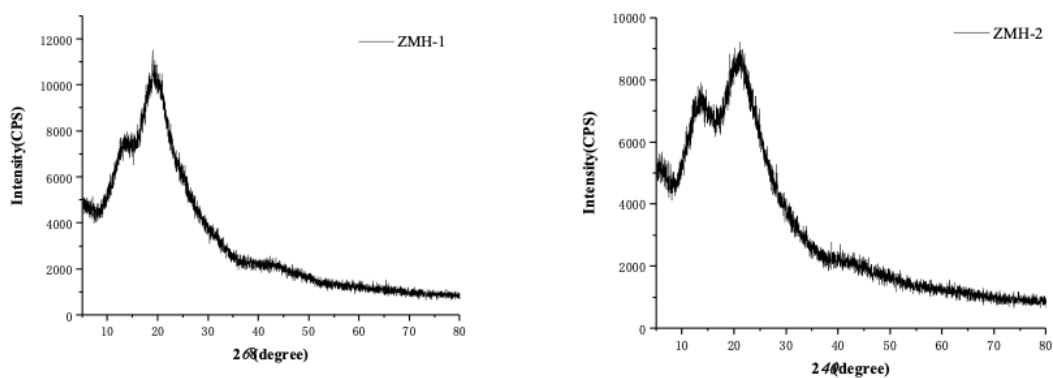


Figure S20. X-ray diffraction patterns of compound **ZMH-1** and **ZMH-2**

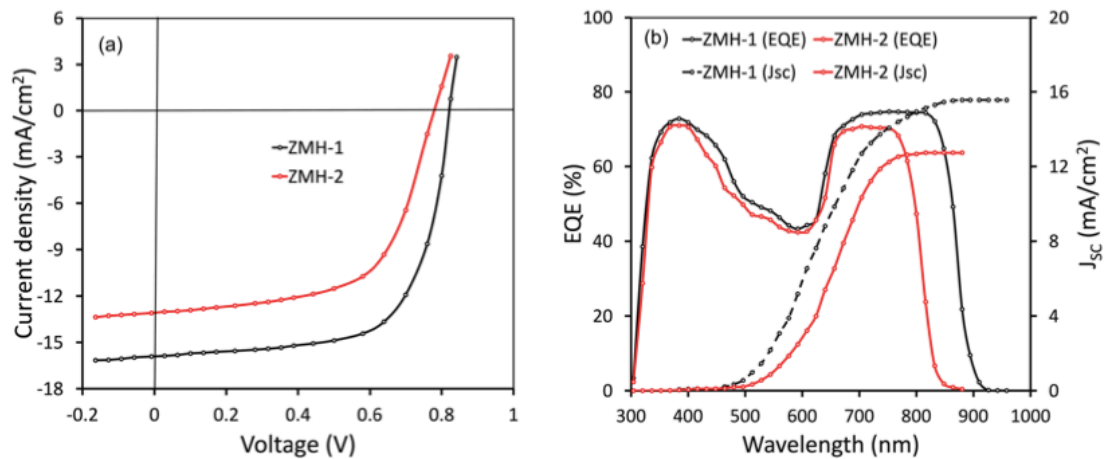


Figure S21. (a) J-V characteristics under illumination and (b) EQE spectra of based on **ZMH-1** and **ZMH-2** as donor and **PC₇₁BM** as acceptor.

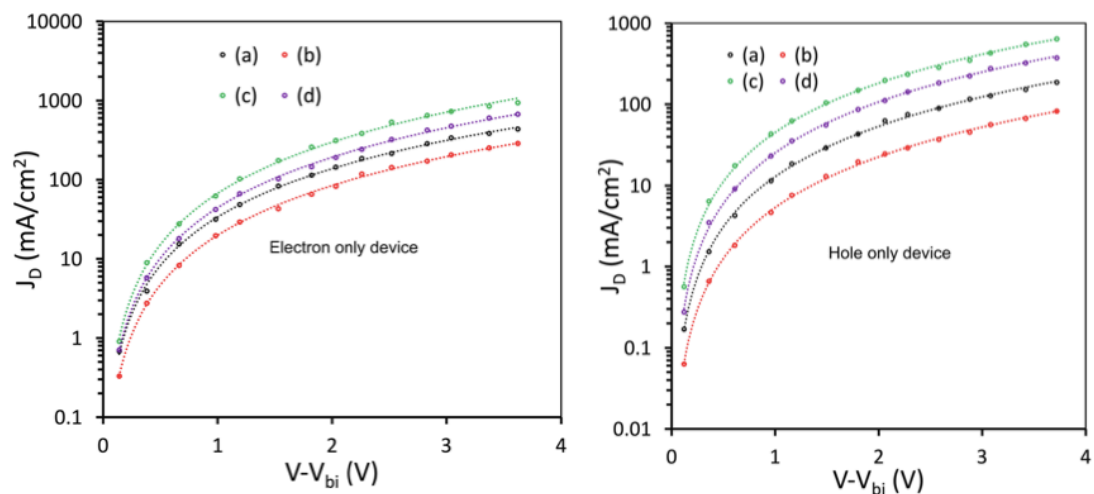


Figure S22. Dark J-V characteristics for the electron (left) and hole (right) only devices and their SCLC fitting using (a) **ZMH-1:IDT-TC**, **ZMH-2:IDT-TC**, **ZMH-1:PC₇₁BM:IDT-TC** and **ZMH-2:PC₇₁BM:IDT-TC** films

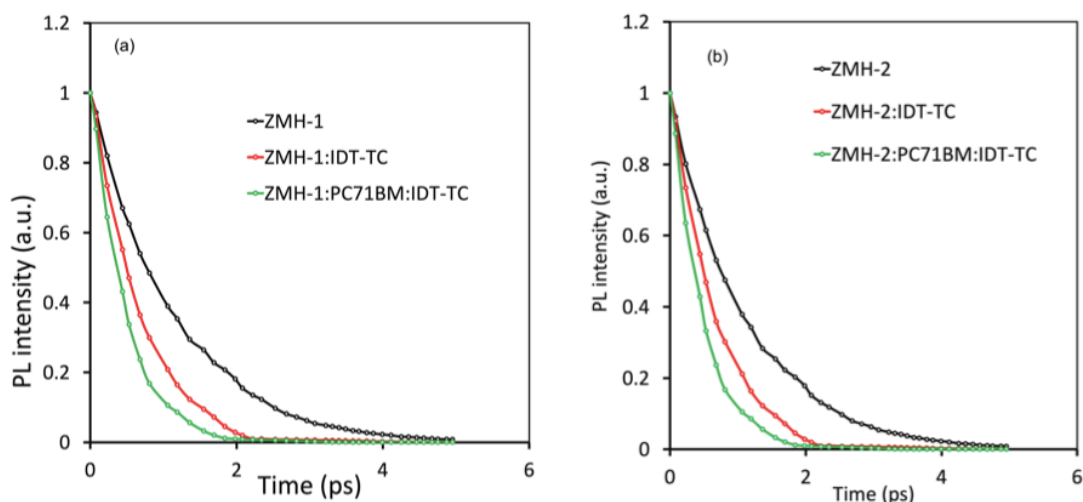


Figure S23. TRPL decay spectra for (a) pristine **ZMH-1** and its binary and ternary blends, and (b) **ZMH-2** and its binary and ternary blends with IDT-TC and PC₇₁BM.

Table S1a. Photovoltaic parameters of the OSCs using **ZMH-1**: IDT-TC BHJ active layer with different weight ratios of **ZMH-1** donor and IDT-TC acceptor as cast using toluene as solvent.

Weight ratio	J _{SC} (mA/cm ²)	V _{OC} (V)	FF	PCE (%)
1:0.2	11.76	0.93	0.557	6.09
1:0.4	12.43	0.94	0.578	6.75
1:0.8	13.54	0.93	0.602	7.58
1:1.2	14.78	0.94	0.612	8.50
1:1.4	14.24	0.93	0.598	7.92

Table S1b. Photovoltaic parameters of the OSCs using **ZMH-2**: IDT-TC BHJ active layer with different weight ratios of **ZMH-2** donor and IDT-TC acceptor as cast using toluene as solvent.

Weight ratio	J _{SC} (mA/cm ²)	V _{OC} (V)	FF	PCE (%)
1:0.2	4.78	0.96	0.41	1.88
1:0.4	5.34	0.96	0.438	2.24
1:0.8	6.83	0.97	0.453	3.00
1:1.2	7.63	0.97	0.462	3.42
1:1.4	7.02	0.96	0.454	3.06

Table S2a. Photovoltaic parameters of OSCs based on ternary **ZMH-1:PC₇₁BM:IDT-TC** with different weight ratios between PC₇₁BM and IDT-TC

Weight ratio	J _{sc} (mA/cm ²)	V _{oc} (V)	FF	PCE (%)
0.2:1.0	16.95	0.93	0.644	10.15
0.4:0.8	18.74	0.92	0.668	11.52
0.6:0.6	17.32	0.91	0.652	10.28

Table S2b. Photovoltaic parameters of OSCs based on ternary **ZMH-2:PC₇₁BM:IDT-TC** with different weight ratios between PC₇₁BM and IDT-TC

Weight ratio	J _{sc} (mA/cm ²)	V _{oc} (V)	FF	PCE (%)
0.2:1.0	15.32	0.93	0.642	9.15
0.4:0.8	16.58	0.94	0.655	10.21
0.6:0.6	16.02	0.94	0.646	9.73